

## Uncooled photodetectors for the 3–5 $\mu\text{m}$ spectral range based on III–V heterojunctions

A. Krier<sup>a)</sup> and W. Suleiman

Department of Physics, Lancaster University, Lancaster LA1 4YB, United Kingdom

(Received 23 May 2006; accepted 30 June 2006; published online 23 August 2006)

The design, fabrication, and characterization of heterojunction photodiodes for room temperature operation in the mid-infrared (3–5  $\mu\text{m}$ ) spectral range is described. Devices appropriate for carbon dioxide detection have been developed and studied. The authors report on the improvements obtained by increasing buffer layer thickness and also by using a blocking barrier to reduce leakage current. © 2006 American Institute of Physics. [DOI: 10.1063/1.2337995]

There are many applications in industrial and environmental monitoring of trace gases and vapors, which could benefit from the provision of uncooled mid-infrared photodetectors and focal plane arrays. For example, detection of methane and hydrocarbons in mines and on oil rigs and monitoring of CO and CO<sub>2</sub> in car exhausts and in heating and ventilation applications all require efficient and inexpensive photodetectors. High speed, sensitive mid-infrared detectors are also required for remote sensing employing semiconductor based lasers, to enable free space optical communications with high security, and also for the monitoring of biomedical analytes. Meanwhile, limitations on payload, space, and prime power on aircraft put a premium on lightweight, compact, power-efficient sensor systems and compact imaging sensors need smaller, lighter, and lower cost focal plane arrays. There are currently no high efficiency mid-infrared photodiodes which operate in the 3–5  $\mu\text{m}$  atmospheric spectral window at room temperature and which can easily meet these needs. It is therefore necessary to develop efficient and reliable mid-infrared photodetectors that can work at room temperature. Recently several different approaches have emerged to address this problem based on quantum nanostructures including: InGaAs/InAlAs quantum well intersubband photodetectors (QWIPs),<sup>1</sup> InAs/GaSb strained layer superlattices (SLSs),<sup>2</sup> and structures based on quantum dots (QDs) or quantum dots in a quantum well. Using sufficiently high band offsets QWIPs can achieve mid-infrared wavelength operation near room temperature, but cannot receive radiation at normal incidence. QD detectors overcome this problem, but require high dot density to obtain sufficient photon absorption. Each of these structures requires careful epitaxial growth, sometimes requiring precise control of many layers, and is likely to result in devices which are expensive to manufacture. In this work we report on a simpler approach based on a specially optimized InAsSb/InAsSbP heterostructure photodiode grown by liquid phase epitaxy (LPE).

Liquid phase epitaxy is an attractive option for the development of practical mid-infrared photodetectors. The technology is inexpensive and can yield high-quality material with excellent quantum efficiency since growth occurs near thermodynamic equilibrium. In many cases the results obtained using bulk heterostructures are often better than some of the emerging quantum nanostructures which are un-

der development. By using the InAsSbP/InAs system it is possible to fabricate heterostructure *p-i-n* diodes, employing InAsSbP as a wide gap window to improve transparency. Using this approach in previous work for 3.3  $\mu\text{m}$ ,<sup>3</sup> we obtained a spectral detectivity ( $D^*$ ) of  $1 \times 10^{10} \text{ cm Hz}^{1/2} \text{ W}^{-1}$ . The longer wavelengths can be accessed from the InAs substrate using stepped buffer layers to accommodate the lattice mismatch. Previously we obtained good sensitivity in the 4.6  $\mu\text{m}$  spectral range using an intermediate composition InAs<sub>0.94</sub>Sb<sub>0.06</sub> buffer layer.<sup>4</sup> In the present work we report on the improvements obtained by (a) increasing buffer layer thickness and (b) using a blocking barrier to reduce leakage current.

The *p-i-n* photodiode structure used in our investigation is shown schematically in Fig. 1. All the epitaxial layers were grown by LPE at  $\sim 552^\circ\text{C}$  using a conventional horizontal sliding graphite boat in an ultrapure hydrogen atmosphere. Zn-doped (100) *p*-type InAs substrates were used with a carrier concentration of  $2 \times 10^{18} \text{ cm}^{-3}$ . The precursors for the growth melts were undoped polycrystalline InAs, InSb, InP, and 7N's pure indium metal. The *p*-type InAs<sub>0.55</sub>Sb<sub>0.15</sub>P<sub>0.30</sub> was doped to  $4 \times 10^{18} \text{ cm}^{-3}$  with Zn, whereas the *n*-type InAs<sub>0.55</sub>Sb<sub>0.13</sub>P<sub>0.30</sub> layer was unintentionally doped and had a residual carrier concentration of  $1 \times 10^{17} \text{ cm}^{-3}$ . In order to remove impurities from the InAs<sub>0.89</sub>Sb<sub>0.11</sub> active region, this melt was baked out for 20 h at  $750^\circ\text{C}$  before the other melts were loaded into the boat. Then, to purify it still further, 0.002 mol % Gd was added to the active region melt to act as an impurity gettering agent during subsequent epitaxy. Hall measurements revealed that this procedure reduced the residual carrier concentration in the active region to  $< 2 \times 10^{16} \text{ cm}^{-3}$ . The resulting epitaxial *p-i-n* structures were processed into 1 mm diameter mesa-

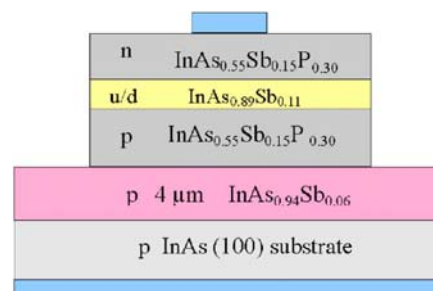


FIG. 1. (Color online) Diagram of the epilayer structure of the mesa-etched photodiode.

<sup>a)</sup>Electronic mail: a.krier@lancaster.ac.uk

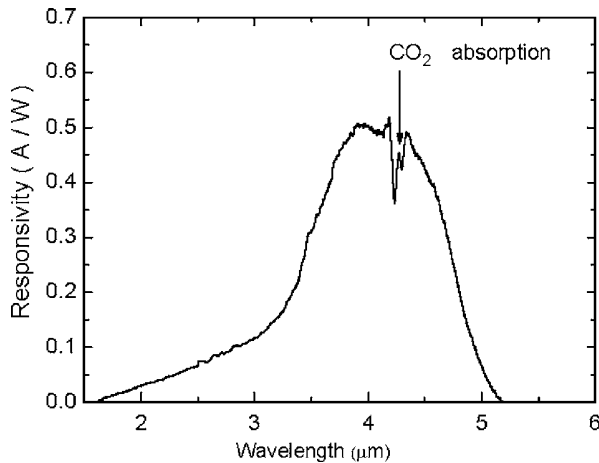


FIG. 2. Room temperature photoresponse obtained from a 1 mm diameter heterostructure photodiode grown by LPE.

etched photodiodes using conventional photolithography and processing techniques. Ohmic contacts were formed by thermal evaporation of Au to provide Ohmic dot contacts, and finally, the chips were mounted onto T0-46 headers for testing. No attempt was made to passivate the surfaces or include an antireflection coating at this stage of our work, and all subsequent results refer to uncoated unpassivated detectors. The detectivity  $D^*$  and spectral response were measured using a chopping frequency of 180 Hz and a blackbody temperature of 1100 K. The recorded spectrum was corrected for system response using a Heimann LHi-807-G11 pyroelectric detector with a flat response.

A typical corrected spectral response measured from one of the detectors at 300 K is shown in Fig. 2, where the peak responsivity is obtained near 4  $\mu\text{m}$ . The atmospheric absorption at 4.2  $\mu\text{m}$  from residual  $\text{CO}_2$  in the optical path is clearly evident. The response extending towards short wavelengths is due to absorption in the quaternary window layer.

Lattice mismatch in heterostructure devices generates threading dislocations, which need to be controlled if the active region is to have good quantum efficiency. We investigated the effect of the buffer layer thickness on the etch pit

density (EPD) in the various layers of the device structure. As shown in Fig. 3, increasing the buffer layer thickness reduced the dislocation density by one order of magnitude. Region A is the entanglement region which corresponds to the highest dislocation densities obtained close to the buffer/substrate interface. These dislocations have Burgers vectors parallel to the interface between the substrate and the buffer layer. With increasing thickness of the buffer layer, the EPD scaled as  $1/d$  (see inset) in good agreement with previous works.<sup>5,6</sup> The observed  $1/d$  dependence can be understood from a binary recombination law. The probability that two threading dislocations meet during growth in order to annihilate is proportional to  $\rho^2$ , where  $\rho$  is the density of threading ends. If  $D(x)$  is the number of threading dislocations per unit area, the rate at which dislocations disappear by recombination will then be proportional to the square of their concentration, so we can write

$$dD/dx = -aD^2, \quad (1)$$

where  $a$  is a constant and has the dimensions of length. Integration yields

$$D(x) = D(0)/(1 + D(0)ax) \sim 1/ax, \quad (2)$$

where  $D(0)$  is the primary threading dislocation density, and where the asymptotic limit refers to the situation sufficiently far from the interface that the majority of dislocations have recombined. The physical mechanisms responsible for threading dislocation reduction in region B are reactions between them that lead to either annihilation of threading segments with antiparallel Burgers vectors or reactions in which two threading dislocations combine to form one (referred to as fusion reactions). These reactions are only possible if the threading dislocations have a minimum separation distance smaller than a physically prescribed interaction distance referred to as the annihilation radius  $r_A$  or the fusion radius  $r_F$ .<sup>7,8</sup> By increasing the buffer layer thickness  $d$ , the threading dislocations are inclined and their intersection point with the free surface moves. Thus, without glide, there is effective lateral motion of the threading dislocations such that they fall within an annihilation or fusion radius of one to another. We found that by using a 9  $\mu\text{m}$  thick buffer layer it was possible

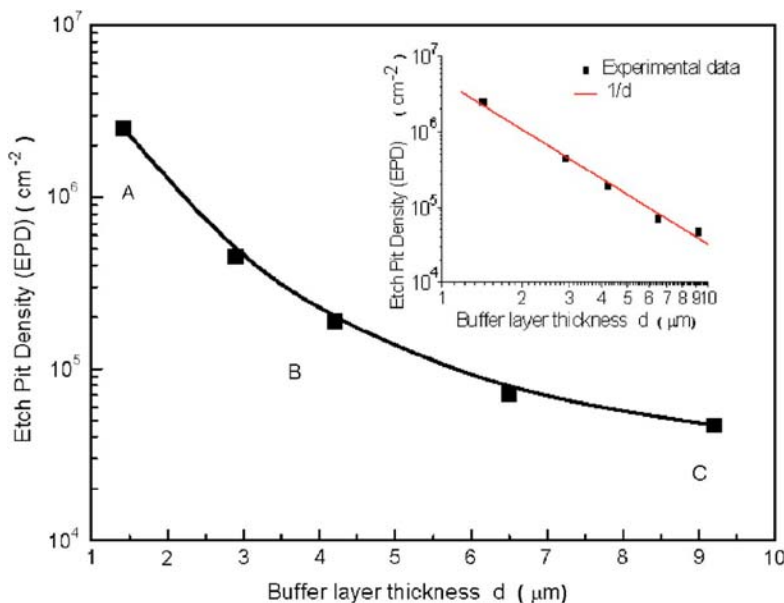


FIG. 3. (Color online) Effect of increasing buffer layer thickness on the etch pit density in the active region of a 4.6  $\mu\text{m}$   $p-i-n$  photodiode. The inset shows a log-log plot which reveals a  $1/d$  dependence on buffer layer thickness.

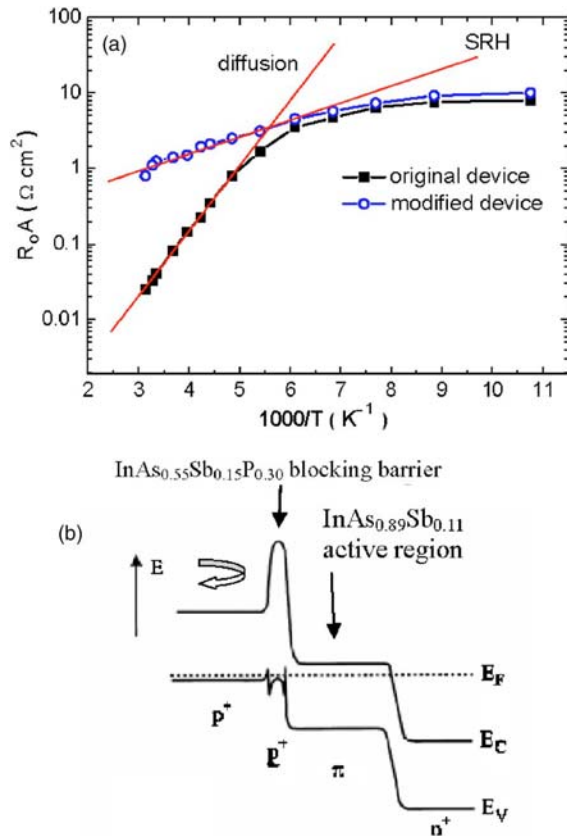


FIG. 4. (Color online) (a) Resistance area product ( $R_0A$ ) vs  $1/T$  for one of the photodiodes. The solid squares show that diffusion current dominates the dark current at room temperature. The open circles represent the improvement in performance using a thin barrier. (b) The band diagram of the detector with a blocking barrier.

to reach the saturation region C and reduce the EPD back to the level in the InAs substrate. Over the range of buffer layer thickness from 1 to 9  $\mu\text{m}$ , the  $R_0A$  increased by a factor of  $\sim 2$ , with a corresponding decrease in the dark current. In addition, there was a corresponding improvement in the responsivity of 2.7 times giving an increase of approximately four times in the  $D^*$ .

An investigation of the leakage current in these detectors revealed that the  $R_0A$  was dominated by generation-recombination current at low temperature, and by diffusion current at room temperature as shown in Fig. 4. The source of the diffusion current was found to originate from electron generation within the wide gap InAsSbP layer. By following the work of Ashley *et al.*<sup>9</sup> and progressively reducing the thickness of this layer, it was possible to realize a thin

(<250 nm) blocking barrier and reduce the contribution to diffusion current generated in this layer. The InAsSbP layer also serves as an effective barrier to prevent leakage into the active region from the buffer layer beneath it. Overall this increased the  $R_0A$  by a factor of 16 and gave a corresponding increase of four times in  $D^*$ . By combining the improvement in active layer quality from the thicker buffer layer mentioned above with that from the blocking barrier, we achieved a peak  $D^*$  of  $3.5 \times 10^9 \text{ cm Hz}^{1/2} \text{ W}^{-1}$  for mesa-etched detectors with a 1 mm diameter active area operating at 4  $\mu\text{m}$ .

In summary, we have demonstrated that using LPE growth efficient uncooled photodetectors for the mid-infrared spectral range can be fabricated. The performance depends on the control of threading dislocations and minimization of the diffusion current as well as the reduction of residual impurity concentration in the active region. We have previously reported high-quality lattice matched  $\text{InAs}_{0.91}\text{Sb}_{0.09}$  epilayers grown by LPE from Sb-rich melts onto lattice matched GaSb substrates with efficient photoluminescence and good electrical transport properties.<sup>10</sup> Although growth from Sb solution onto GaSb avoids the problem of substrate erosion during epilayer nucleation, the associated thermodynamics restricts the epitaxy to a relatively narrow range of experimental growth conditions. So far we have obtained superior detector performance from InAsSb  $p$ - $i$ - $n$  photodiodes fabricated on InAs substrates using a stepped buffer layer. Further improvements in  $D^*$  could readily be obtained from smaller devices, since leakage current scales with area. However, for sensor applications which require a large area photovoltaic detector with a large field of view, the present work represents a useful result.

The authors wish to thank Kidde PLC for continued support of this work. They also wish to thank D. Campbell and G. Crook for valuable technical assistance.

- <sup>1</sup>K. T. Lai and S. K. Haywood, *Semicond. Sci. Technol.* **21**, 813 (2006).
- <sup>2</sup>F. Fuchs, L. Buerkle, R. Hamid, and N. Herres, *Proc. SPIE* **4288**, 171 (2001).
- <sup>3</sup>A. Krier, H. H. Gao, and V. V. Sherstnev, *Appl. Phys. Lett.* **77**, 872 (2000).
- <sup>4</sup>A. Krier, H. H. Gao, and Y. Mao, *Semicond. Sci. Technol.* **13**, 950 (1998).
- <sup>5</sup>H. Kroemer, T. Y. Liu, and P. M. Petroff, *J. Cryst. Growth* **95**, 96 (1989).
- <sup>6</sup>J. S. Speck, M. A. Brewer, G. Beltz, A. E. Romanov, and W. Pompe, *J. Appl. Phys.* **80**, 3808 (1996).
- <sup>7</sup>A. A. Kusov and V. I. Vladimirov, *Phys. Status Solidi B* **138**, 135 (1986).
- <sup>8</sup>M. Y. Martisov and A. E. Romanov, *Sov. Phys. Solid State* **32**, 1101 (1990).
- <sup>9</sup>T. Ashley, A. B. Dean, C. T. Elliott, A. D. Johnson, G. J. Pryce, A. M. White, and C. R. Whitehouse, *Semicond. Sci. Technol.* **8**, S386 (1993).
- <sup>10</sup>Y. Mao and A. Krier, *J. Cryst. Growth* **133**, 108 (1993).